PRAMANA
— journal of
physics

Vol. 86, No. 1
January 2016
pp. 3–17

Stretched flow of Carreau nanofluid with convective boundary condition

T HAYAT[1,2], M WAQAS[1], S A SHEHZAD[3,*] and A ALSAEDI[2]

[1]Department of Mathematics, Quaid-i-Azam University 45320, Islamabad 44000, Pakistan
[2]Nonlinear Analysis and Applied Mathematics (NAAM) Research Group, Faculty of Science, King Abdulaziz University, P.O. Box 80257, Jeddah 21589, Saudi Arabia
[3]Department of Mathematics, Comsats Institute of Information Technology, Sahiwal 57000, Pakistan
*Corresponding author. E-mail: ali_qau70@yahoo.com

MS received 16 May 2015; accepted 1 October 2015
DOI: 10.1007/s12043-015-1137-y; ***e*Publication:** 12 December 2015

Abstract. The steady laminar boundary layer flow of Carreau nanofluid over a stretching sheet is investigated. Effects of Brownian motion and thermophoresis are present. Heat transfer is characterized using convective boundary condition at the sheet. The governing partial differential equations are reduced into a set of nonlinear ordinary differential equations through suitable transformations. Results of velocity, temperature and concentration fields are computed via homotopic procedure. Numerical values of skin-friction coefficient, local Nusselt and Sherwood numbers are computed and discussed. A comparative study with existing solutions in a limiting sense is made.

Keywords. Steady flow; Carreau nanofluid; convective condition; stretching sheet.

PACS Nos 47.50.−d; 02.30.Hq; 02.30.Jr

1. Introduction

Flows of nanofluids have attracted the continuous attention of researchers. It is due to the fact that conventional heat transfer fluids, including oil, water and ethylene glycol mixture are poor heat conductors as the thermal conductivities of these fluids play important roles on the heat transfer coefficient between the heat transfer medium and the heat transfer surface. Therefore, numerous methods have been adopted to improve thermal conductivity of these fluids by suspending nano/micro or larger-sized particles in liquids [1]. An innovative technique to improve heat transfer is to introduce nanoscale particles to the base fluid [2]. Nanotechnology has been widely used in industry as materials of nanometre-size possess unique physical and chemical properties. Nanoscale particle-added fluids are called nanofluids which were used first by Choi [2]. Choi *et al* [3] showed that the addition of a small amount (less than 1% by volume) of nanoparticles

to conventional heat transfer liquids increases the thermal conductivity of the fluid almost twice. Khanafer *et al* [4] were among the first to have examined heat transfer performance of nanofluids inside an enclosure by taking into account the solid-particle dispersion. The basic aim of nanomaterials is to manipulate the structure of matter at the molecular level with the goal for innovation in virtually every industry and public endeavour including biological sciences, physical sciences, electronics cooling, transportation, the environment and national security. Some numerical and experimental studies relevant to nanofluids can be seen in refs [5–15].

The study of flow over a stretching sheet has generated much interest in recent years due to its important contributions, especially in many engineering processes and industries. Some applications in this direction include the aerodynamic extrusion of plastic sheets, glass-fibre production, condensation process of metallic plate in a cooling bath, paper production etc. It seems that Crane [16] was the first to report analytical solution for the laminar boundary layer flow past a stretching sheet. He constructed an exact solution for the arising nonlinear problem. After this pioneering work, the study of the flow of fluid over a stretching sheet has received wide attention among the researchers. Effects of Joule heating and thermophoresis in stretched flow with convective boundary conditions have been investigated by Hayat *et al* [17]. Mukhopadhyay *et al* [18] presented magnetohydrodynamic (MHD) flow and heat transfer over a stretching sheet with variable fluid viscosity. Bhattacharyya and Layek [19] showed the behaviour of solute distribution in MHD boundary layer flow, past a stretching sheet. Very recently, Khan *et al* [20] investigated the three-dimensional flow of an Oldroyd-B nanofluid over a stretching surface with heat generation/absorption.

Recently, investigations of boundary layer flow subject to convective heat transfer have gained much interest among the researchers. It is due to its importance in technological and manufacturing processes. Convective heat transfer plays a vital role in many engineering problems involving both metals and polymer sheets, packed sphere beds, high-performance chemical catalytic, heat exchange between sensible heat storage beds, electrochemical processes, insulation of nuclear reactors, etc. Aziz [21] initiated the concept of convective boundary condition. He discussed the boundary layer flow of viscous fluid over a flat plate subjected to convective surface condition. This problem was then extended by Bataller [22] by considering the Blasius and Sakiadis flows, over a convectively heated surface with thermal radiation. Ishak [23] obtained similarity solutions for the steady laminar boundary layer flow over a permeable plate with a convective boundary condition. Makinde and Aziz [24] investigated numerically, the effect of a convective boundary condition in the two-dimensional boundary layer flows of nanofluid past a stretching sheet. Mixed convection radiative flow of Maxwell fluid near a stagnation point with convective boundary condition was investigated by Hayat *et al* [25].

The range of non-Newtonian fluids is very large because of their presence in the engineering and industrial processes. Such fluids are quite commonly used in the manufacture of coated sheets, foods, optical fibres, drilling muds, plastic polymers, etc. It is well known that all the non-Newtonian fluids, because of their diverse characteristics, cannot be described by a single constitutive relationship. Hence several models of non-Newtonian fluids have been suggested. The governing equations for the flows of non-Newtonian fluids, in general, are much complicated, more nonlinear and of higher order than the Navier–Stokes equations. Unlike power-law fluid, the Carreau model is one of

the non-Newtonian fluid models for which constitutive relationship holds at both low and high shear rates. Due to this fact, it has achieved wider acceptance at present. Hayat *et al* [26] investigated the boundary layer flow of Carreau fluid over a convectively heated stretching sheet. Numerical solution of the resulting differential system is obtained by the homotopy analysis method (HAM). Ali and Hayat [27] discussed the peristaltic transport of Carreau fluid in an asymmetric channel. Heat and mass transfer in hydromagnetic flow of Carreau fluid past a vertical porous plate with thermal radiation and thermal diffusion is addressed by Olajuwon [28]. Tshehla [29] studied the flow of Carreau fluid down an inclined free surface.

The present communication model analyses the flow of Carreau fluid over a stretching sheet in the presence of nanoparticles. Problem formulation consists of Brownian motion and thermophoresis effects. The resulting nonlinear system is reduced to the ordinary differential system. The homotopy analysis method is adopted in the computation of the nonlinear analysis [30–40]. The developed convergent series solutions are sketched and analysed very carefully.

2. Governing problems

We consider the steady two-dimensional boundary layer flow of a Carreau nanofluid bounded by a permeable stretching surface at $y = 0$. The x- and y-axes are taken along and normal to the stretched surface, respectively. We denote C_w as the value of nanoparticle fraction (C) at the surface. Temperature of the sheet surface (to be determined later) is the result of a convective heating process which is characterized by temperature T_f and heat transfer coefficient h. The extra stress tensor for the Carreau fluid is given by

$$\tau_{ij} = [\eta_0 \left(1 + (\lambda\dot{\gamma})^2\right)^{(n-1)/2}]\dot{\gamma}_{ij}, \tag{1}$$

where τ_{ij} is the extra stress tensor, η_0 is the zero shear rate viscosity, λ is the time constant, n is the power law index and $\dot{\gamma}$ is defined as follows:

$$\dot{\gamma} = \sqrt{\frac{1}{2}\sum_i \sum_j \dot{\gamma}_{ij}\dot{\gamma}_{ji}} = \sqrt{\frac{1}{2}\Pi}. \tag{2}$$

Here Π is the second invariant strain tensor. The boundary layer equations governing the present flow consideration are

$$\frac{\partial u}{\partial x} + \frac{\partial v}{\partial y} = 0, \tag{3}$$

$$\begin{aligned} u\frac{\partial u}{\partial x} + v\frac{\partial u}{\partial y} = {} & \nu\frac{\partial^2 u}{\partial y^2}\left[1 + \left(\frac{n-1}{2}\right)\lambda^2\left(\frac{\partial u}{\partial y}\right)^2\right] \\ & + \nu(n-1)\lambda^2\left[\frac{\partial^2 u}{\partial y^2}\left(\frac{\partial u}{\partial y}\right)^2\right] \\ & \times\left[1 + \left(\frac{n-3}{2}\right)\lambda^2\left(\frac{\partial u}{\partial y}\right)^2\right], \end{aligned} \tag{4}$$

$$u\frac{\partial T}{\partial x}+v\frac{\partial T}{\partial y}=\alpha_m\frac{\partial^2 T}{\partial y^2}+\tau\left(D_{\mathrm{B}}\frac{\partial C}{\partial y}\frac{\partial T}{\partial y}+\frac{D_{\mathrm{T}}}{T_\infty}\left(\frac{\partial T}{\partial y}\right)^2\right), \tag{5}$$

$$u\frac{\partial C}{\partial x}+v\frac{\partial C}{\partial y}=D_{\mathrm{B}}\frac{\partial^2 C}{\partial y^2}+\frac{D_{\mathrm{T}}}{T_\infty}\frac{\partial^2 T}{\partial y^2}. \tag{6}$$

Here u and v are the velocity components parallel to the x- and y-axes, $\nu=(\mu/\rho)$ is the kinematic viscosity, ρ is the fluid density, T is the fluid temperature, D_{B} is the Brownian diffusion coefficient, D_{T} is the thermophoretic diffusion coefficient, α_m is the thermal diffusivity of ordinary fluid, τ is the ratio of effective heat capacity of the nanoparticle material and the heat capacity of ordinary fluid.

The associated boundary conditions are given by

$$u=u_w(x)=cx,\quad v=0,\quad -K\frac{\partial T}{\partial y}=h\left(T_f-T\right),\quad C=C_w\quad \text{at } y=0, \tag{7}$$

$$u\to 0,\quad T\to T_\infty,\quad C\to C_\infty\quad \text{as } y\to\infty. \tag{8}$$

Introducing

$$\eta=y\sqrt{\frac{c}{\nu}},\quad u=cxf'(\eta),\quad v=-\sqrt{c\nu}\,f(\eta),$$

$$\theta(\eta)=\frac{T-T_\infty}{T_\infty},\quad \frac{C-C_\infty}{C_w-C_\infty}, \tag{9}$$

eq. (3) is automatically satisfied and eqs (4)–(8) give

$$f'''\left(1+\left(\frac{n-1}{2}\right)\lambda_1 f''^2\right)+2\left[\left(\frac{n-1}{2}\right)\lambda_1 f''^2\right]\left[1+\left(\frac{n-3}{2}\right)\lambda_1 f''^2\right], \tag{10}$$

$$\theta''+\mathrm{Pr}(N_{\mathrm{b}}\theta'\phi'+N_{\mathrm{t}}\theta'^2)=0, \tag{11}$$

$$\phi''+\mathrm{PrLe}\ f\phi'+\frac{N_{\mathrm{t}}}{N_{\mathrm{b}}}\theta''=0, \tag{12}$$

$$f(0)=0,\quad f'(0)=1,\quad f'(\infty)=0, \tag{13}$$

$$\theta(\eta)=-\gamma\left[1-\theta\left(\eta\right)\right]\quad \text{at } \eta=0,\quad \theta(\eta)=0\quad \text{at } \eta=\infty, \tag{14}$$

$$\phi(0)=1,\quad \phi\left(\infty\right)=0, \tag{15}$$

where prime denotes differentiation with respect to η. Material parameter λ_1, Prandtl number Pr, thermophoresis parameter N_{t}, Brownian motion parameter N_{b}, Lewis number Le and Biot number γ are given by

$$\lambda_1=\lambda c^2,\quad \mathrm{Pr}=\frac{\nu}{\alpha_m},\quad N_{\mathrm{t}}=\frac{\tau D_{\mathrm{T}}\left(T_w-T_\infty\right)}{T_\infty\nu},$$

$$N_{\mathrm{b}}=\frac{\tau D_{\mathrm{B}}\left(\phi_w-\phi_\infty\right)}{\nu},\quad \mathrm{Le}=\frac{\alpha_m}{D_{\mathrm{B}}},\quad \gamma=\frac{h}{k}\sqrt{\frac{\nu}{c}}. \tag{16}$$

The skin fraction coefficient C_{fx}, local Nusselt number Nu_x and local Sherwood number Sh_x can be expressed as follows:

$$C_{fx} = \frac{\tau_w}{\frac{1}{2}\rho u_w^2}, \tag{17}$$

$$\mathrm{Nu}_x = \frac{x\,(\partial T/\partial y)_{y=0}}{(T_w - T_\infty)}, \quad \mathrm{Sh}_x = \frac{x\,(\partial C/\partial y)_{y=0}}{(C_w - C_\infty)}, \tag{18}$$

where

$$\tau_w = \eta_0 \left(\left(\frac{\partial u}{\partial y} \right) + \left(\frac{n-1}{2} \right) \lambda^2 \left\{ \begin{array}{l} (\partial u/\partial y)\,(\partial u/\partial x)^2 + \\ 3(\partial v/\partial x)\,(\partial u/\partial y)^2 \end{array} \right\} \right)_{y=0}. \tag{19}$$

In dimensionless forms, the above expressions are reduced to the following definitions:

$$C_f = \mathrm{Re}^{-1/2} \left(1 + \left(\frac{n-1}{2} \right) \lambda_1 \right) f''(0),$$

$$\mathrm{Nu}_x/\mathrm{Re}_x^{1/2} = -\theta'(0), \quad \mathrm{Sh}_x/\mathrm{Re}_x^{1/2} = -\phi'(0), \tag{20}$$

where $\mathrm{Re}_x = cx^2/\nu$ is the local Reynolds number.

3. Series solutions

Initial approximations and auxiliary linear operators for homotopic solutions can be chosen as follows:

$$f_0(\eta) = \left(1 - \mathrm{e}^{-\eta}\right), \quad \theta_0(\eta) = \frac{\gamma}{1+\gamma} \exp(-\eta), \quad \phi_0(\eta) = \exp(-\eta), \tag{21}$$

$$L_f = f''' - f', \quad L_g = g'' - g', \quad L_\theta = \theta'' - \theta. \tag{22}$$

Here the properties satisfied by the chosen operators are

$$L_f(C_1 + C_2\mathrm{e}^{\eta} + C_3\mathrm{e}^{-\eta}) = 0, \quad L_g(C_4\mathrm{e}^{\eta} + C_5\mathrm{e}^{-\eta}) = 0,$$

$$L_\phi(C_6\mathrm{e}^{\eta} + C_7\mathrm{e}^{-\eta}) = 0, \tag{23}$$

where C_i, $i = 1{-}7$, indicate arbitrary constants.

The corresponding problems at the zeroth order are given in the following forms:

$$(1-p)\,L_f[\hat{f}(\eta;p) - f_0(\eta)] = p\hbar_f \mathbf{N}_f[\hat{f}(\eta;p)], \tag{24}$$

$$(1-p)\,L_\theta[\hat{\theta}(\eta;p) - \theta_0(\eta)] = p\hbar_\theta \mathbf{N}_\theta[\hat{f}(\eta;p),\ \hat{\theta}(\eta,p),\ \hat{\phi}(\eta,p)], \tag{25}$$

$$(1-p)\,L_\phi[\hat{\phi}(\eta;p) - \phi_0(\eta)] = p\hbar_\phi \mathbf{N}_\phi[\hat{f}(\eta;p),\ \hat{\theta}(\eta,p),\ \hat{\phi}(\eta,p)], \tag{26}$$

$$\hat{f}(0;p) = 0, \quad \hat{f}'(0;p) = 1, \quad \hat{f}'(\infty;p) = 0, \quad \hat{\theta}'(0,p) = -\gamma\,(1+\theta\,(0)),$$
$$\hat{\theta}(\infty,p) = 0, \quad \hat{\phi}(0,p) = 1, \quad \hat{\phi}(\infty,p) = 0, \tag{27}$$

$$N_f[\hat{f}(\eta,p)] = \frac{\partial^3 \hat{f}(\eta,p)}{\partial \eta^3}\left[1+\lambda_1\left(\frac{\eta-1}{2}\frac{\partial^2 \hat{f}(\eta,p)}{\partial \eta^2}\right)\right] + 2\lambda_1\left(\frac{\eta-1}{2}\right)\frac{\partial^2 \hat{f}(\eta,p)}{\partial \eta^2}\left[1+\lambda_1\left(\frac{\eta-1}{3}\right)\frac{\partial^2 \hat{f}(\eta,p)}{\partial \eta^2}\right] - \left(\frac{\partial \hat{f}(\eta,p)}{\partial \eta}\right)^2 + \hat{f}(n,p)\frac{\partial^2 \hat{f}(\eta,p)}{\partial \eta^2}, \tag{28}$$

$$\mathbf{N}_\theta[\hat{f}(\eta,p),\,\hat{\theta}(\eta,p),\,\hat{\phi}(\eta,p)] = \frac{\partial^2 \hat{\theta}(\eta,p)}{\partial \eta^2} + \mathrm{Pr}N_\mathrm{b}\frac{\partial \hat{\theta}(\eta,p)}{\partial \eta}\frac{\partial \hat{\phi}(\eta,p)}{\partial \eta} + \mathrm{Pr}N_\mathrm{t}\frac{\partial^2 \hat{\theta}(\eta,\,p)}{\partial \eta^2}, \tag{29}$$

$$\mathbf{N}_\phi[\hat{f}(\eta,p),\,\hat{\theta}(\eta,p),\,\hat{\theta}(\eta,p)] = \frac{\partial^2 \hat{\phi}(\eta,p)}{\partial \eta^2} + \mathrm{PrLe}\frac{\partial \hat{\phi}(\eta,p)}{\partial \eta} + \frac{N_\mathrm{t}}{N_\mathrm{b}}\frac{\partial^2 \hat{\theta}(\eta,p)}{\partial \eta^2}. \tag{30}$$

Here p is an embedding parameter, $\hbar_f$, $\hbar_\theta$ and $\hbar_\phi$ are the non-zero auxiliary parameters and $\mathbf{N}_f$, $\mathbf{N}_\theta$ and $\mathbf{N}_\phi$ indicate the nonlinear operators. When $p = 0$ and $p = 1$, one has

$$\hat{f}(\eta;0) = f_0(\eta), \quad \hat{\theta}(\eta,0) = \theta_0(\eta), \quad \hat{\phi}(\eta,0) = \phi_0(\eta),$$
$$\hat{f}(\eta;1) = f(\eta), \quad \hat{\theta}(\eta,1) = \theta(\eta), \quad \hat{\phi}(\eta,1) = \phi_0(\eta). \tag{31}$$

By Taylor's series expansion, we have

$$f(\eta,\,p) = f_0(\eta) + \sum_{m=1}^{\infty} f_m(\eta)p^m, \quad f_m(\eta) = \frac{1}{m!}\left.\frac{\partial^m f(\eta;\,p)}{\partial \eta^m}\right|_{p=0}, \tag{32}$$

$$\theta(\eta,\,p) = \theta_0(\eta) + \sum_{m=1}^{\infty} \theta_m(\eta)p^m, \quad \theta_m(\eta) = \frac{1}{m!}\left.\frac{\partial^m \theta(\eta;\,p)}{\partial \eta^m}\right|_{p=0}, \tag{33}$$

$$\phi(\eta,\,p) = \phi_0(\eta) + \sum_{m=1}^{\infty} \phi_m(\eta)p^m, \quad \phi_m(\eta) = \frac{1}{m!}\left.\frac{\partial^m \phi(\eta;\,p)}{\partial \eta^m}\right|_{p=0}, \tag{34}$$

where the convergence of the above series strongly depends upon $\hbar_f$, $\hbar_\theta$ and $\hbar_\phi$. If $\hbar_f$, $\hbar_\theta$ and $\hbar_\phi$ are selected properly, so that eqs (32)–(34) converge at $p = 1$, then we can write

$$f(\eta,p) = f_0(\eta) + \sum_{m=1}^{\infty} f_m(\eta)p^m, \tag{35}$$

$$\theta(\eta,p) = \theta_0(\eta) + \sum_{m=1}^{\infty} \theta_m(\eta)p^m, \tag{36}$$

$$\phi(\eta,\ p) = \phi_0(\eta) + \sum_{m=1}^{\infty} \phi_m(\eta) p^m. \tag{37}$$

The general solutions are given by

$$f_m(\eta) = f_m^*(\eta) + C_1 + C_2 e^{\eta} + C_3 e^{-\eta}, \tag{38}$$

$$\theta_m(\eta) = \theta_m^*(\eta) + C_6 e^{\eta} + C_7 e^{-\eta}, \tag{39}$$

$$\phi_m(\eta) = \phi_m^*(\eta) + C_8 e^{\eta} + C_9 e^{-\eta}, \tag{40}$$

in which f_m^*, θ_m^* and ϕ_m^* indicate the special solutions.

4. Convergence analysis

Clearly, the homotopy analysis solutions depend on the auxiliary parameters $\hbar_f, \hbar_\theta$ and $\hbar_\phi$ which are useful to adjust and control the convergence of series solutions. Hence, to compute the range of admissible values of $\hbar_f, \hbar_\theta$ and $\hbar_\phi$, we display the $\hbar$-curves of the functions $f''(0), \theta'(0)$ and $\phi'(0)$ at 12th-order of approximations (see figure 1). It is found that the admissible values of the auxiliary parameters $\hbar_f, \hbar_\theta$ and $\hbar_\phi$ are $-1.35 \leq \hbar_f \leq -0.30, 1.50 \leq \hbar_\theta \leq -0.35$ and $-1.70 \leq \hbar_\phi \leq -0.30$. The series given by (35)–(37) converge in the whole region of η when $\hbar_f = \hbar_\theta = \hbar_\phi = -0.6$.

5. Results and discussion

In this section, the effects of various physical parameters on the velocity, temperature and nanoparticle concentration are analysed. Figures 2–11 are plotted for this objective. Figure 2 depicts the effect of λ_1 on $f'(\eta)$. By increasing λ_1, the velocity enhances and tends to zero when $n \to \infty$. Effects of power law index on velocity profile

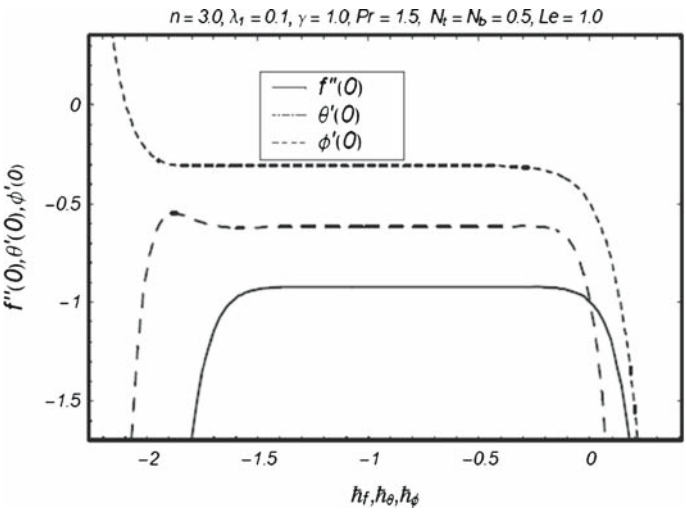

Figure 1. $\hbar$-curves for the functions $f(\eta), \theta(\eta)$ and $\phi(\eta)$.

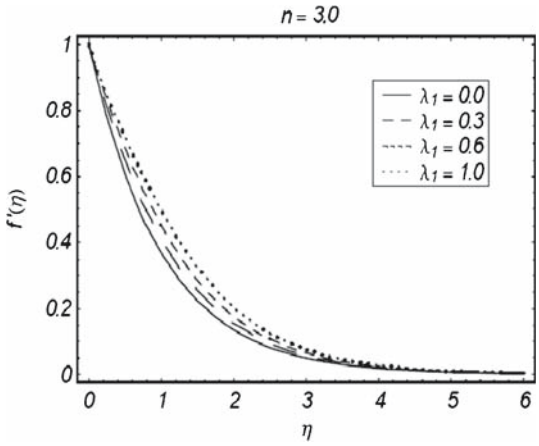

Figure 2. Effects of λ_1 on $f'(\eta)$.

$f'(\eta)$ are depicted in figure 3. We can see that power law index increases the velocity. Effects of Prandtl number Pr on $\theta(\eta)$ are shown in figure 4. The boundary layer corresponding to temperature field decreases when the Prandtl number increases because an increase in Prandtl number gives rise to weaker thermal diffusivity and thinner boundary layer thickness. Larger Prandtl fluids have lower thermal diffusivity and lower Prandtl fluids have higher thermal diffusivity. For smaller Prandtl fluids, we have higher temperature distribution. Figure 5 depicts the influence of Biot number γ on temperature profile $\theta(\eta)$. It is seen that the temperature profile increases rapidly with an increase in γ. Physically, the Biot number depends on the heat transfer coefficient. Higher values of Biot number imply an increase in the heat transfer coefficient. Such an increase in the heat transfer coefficient leads to higher temperature. Influence of thermophoresis parameter N_t on the temperature field is observed in figure 6. Here N_t is an increasing function of temperature profile $\theta(\eta)$ because when N_t is increased, the difference between the wall temperature and reference temperature increases, causing an increase in temperature

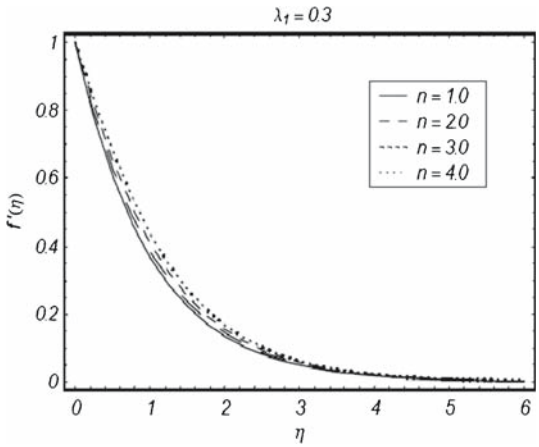

Figure 3. Effects of n on $f'(\eta)$.

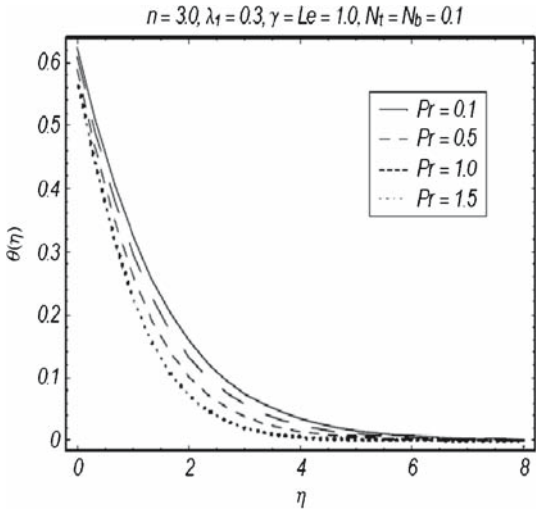

Figure 4. Effects of Pr on $\theta(\eta)$.

profile. Influence of Brownian motion parameter N_b on the temperature field is depicted in figure 7. It is seen that the temperature and thermal boundary layer thickness increase for larger Brownian motion parameter N_b. Physically, this is due to the fact that with an increase of the Brownian motion parameter N_b, the random motion of particle increases resulting in an enhancement of temperature profile.

Figure 8 shows the influence of Pr on concentration profile $\phi(\eta)$. Here, Pr is a decreasing function of concentration profile. Influence of thermophoresis parameter N_t on concentration profile $\phi(\eta)$ is presented in figure 9. Concentration profile $\phi(\eta)$ decreases by increasing N_t. From figure 10, it is observed that concentration profile decreases with

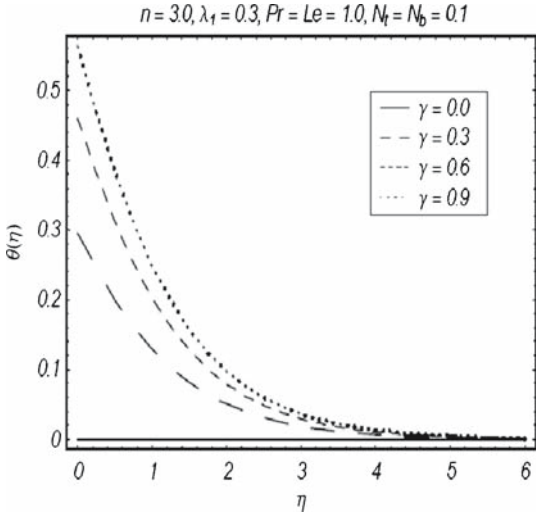

Figure 5. Effects of γ on $\theta(\eta)$.

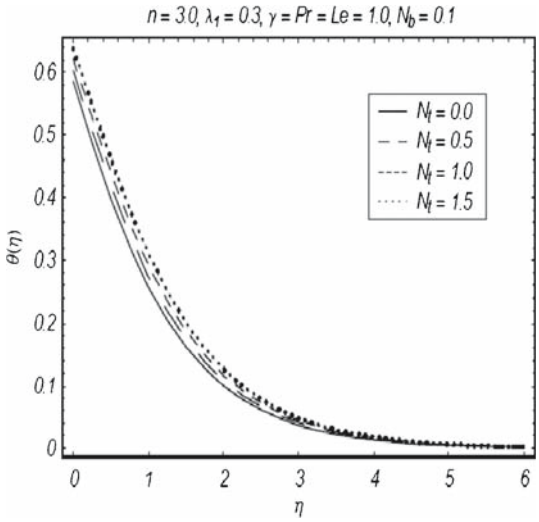

Figure 6. Effects of N_{t} on $\theta(\eta)$.

the increasing values of Brownian motion parameter N_{b}. This is due to the dependency of the concentration on the temperature field and we expect that a lower Brownian motion parameter allows a deeper penetration of concentration. Figure 11 is drawn to see the influence of Lewis number Le on the concentration profile $\phi(\eta)$. As Le is the ratio of momentum to mass diffusivities, an increase in Le leads to a decrease in mass diffusivity and the concentration profile $\phi(\eta)$.

Table 1 ensures the convergence of the involved homotopy solutions. It is found that the convergent solutions for function f is obtained at 10th order of approximations, whereas such a convergence for θ and ϕ is achieved at 25th and 26th order of approximations

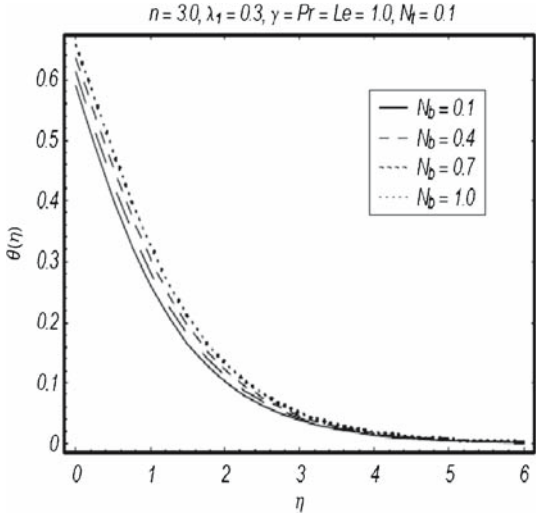

Figure 7. Effects of N_{b} on $\theta(\eta)$.

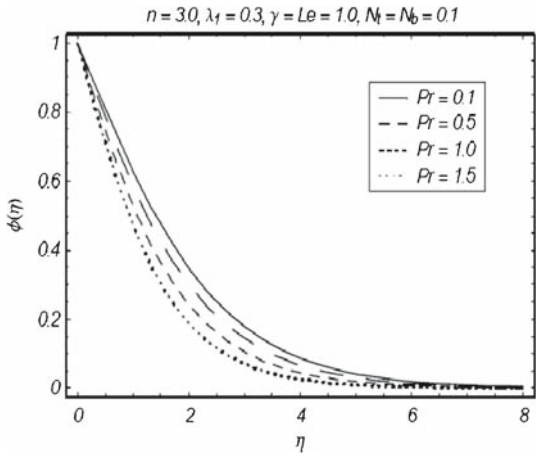

Figure 8. Effects of Pr on (η).

respectively. Table 2 shows the numerical values of skin friction coefficient for different values of λ_1 by taking power law index (n) fixed. It can be seen that by increasing λ_1, the values of skin friction increases. Table 3 is presented for the numerical values of local Nusselt and Sherwood numbers. Larger Biot number γ yields an increase in heat transfer coefficient and heat flux from the sheet. As a result, the wall heat transfer rate increases when γ is increased. Graphical results in figure 4 also show that temperature profile becomes increasingly steeper when γ is increased. This indicates an increase in the wall slope of temperature function. The behaviour of Pr on $-\theta'(0)$ is similar to that of γ in a qualitative sense. Moreover, we can see that the influence of Brownian motion parameter and Lewis number on local Nusselt and Sherwood numbers are qualitatively similar. Tables 4 and 5 give comparison of the present results in a limiting sense with the results already published. It is found that the results obtained in the limiting sense are in excellent agreement with the previous results.

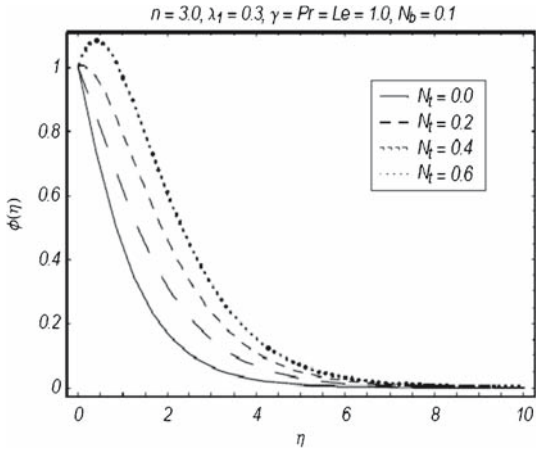

Figure 9. Effects of N_{t} on (η).

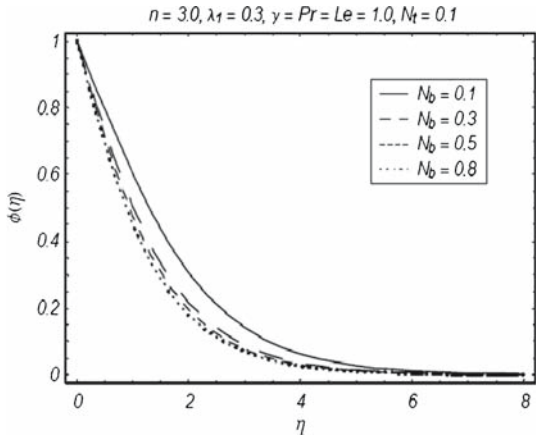

Figure 10. Effects of N_{b} on (η).

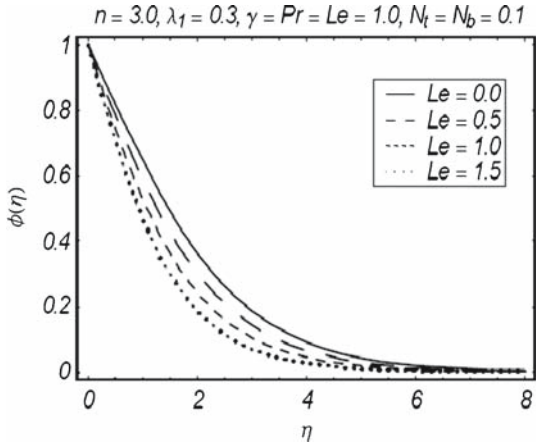

Figure 11. Effects of Le on (η).

Table 1. Convergence of series solutions for different order of approximations when $n = 3.0$, $N_{\mathrm{t}} = N_{\mathrm{b}} = 0.1$, $\mathrm{Pr} = \gamma = \mathrm{Le} = 1.0$ and $\hbar_f = \hbar_\theta = \hbar_\phi = -0.6$.

Order of approximations	$-f''(0)$	$-\theta'(0)$	$-\phi'(0)$
1	0.83500	0.44250	0.65000
5	0.81129	0.37254	0.40743
10	0.81140	0.36236	0.38099
15	0.81140	0.36153	0.37338
20	0.81140	0.36149	0.37171
25	0.81140	0.36148	0.37150
26	0.81140	0.36148	0.37149
35	0.81140	0.36148	0.37149
45	0.81140	0.36148	0.37149

Table 2. Values of skin friction coefficient $(\mathrm{Re}_x)^{1/2} C_{f_x}$ for different values of λ_1 when $n = 3.0$.

λ_1	$-f''(0)$
0.0	1.0000
0.1	1.0158
0.2	1.0347
0.3	1.0548
0.4	1.0755
0.5	1.0962

Table 3. Values of local Nusselt $-\theta'(0)$ for different values of the parameters N_b, N_t, Le, Pr and γ when $\lambda_1 = 0.2$ and $n = 3.0$.

N_b	N_t	Le	Pr	γ	$-\theta'(0)$	$-\phi'(0)$
0.2	0.1	1.0	1.0	1.0	0.34677	0.48725
0.4					0.32320	0.54883
0.6					0.29982	0.56925
0.1	0.0				0.36297	0.59923
	0.1				0.35857	0.36402
	0.2				0.35416	0.13650
	0.1	1.1			0.35797	0.40934
		1.2			0.35742	0.45252
		1.3			0.35693	0.49376
		1.3	0.7		0.30903	0.36219
			0.8		0.32641	0.40722
			0.9		0.34260	0.45130
			1.0	1.2	0.37920	0.48024
				1.3	0.38847	0.47461
				1.4	0.39680	0.46956

Table 4. Comparison of values of $-\theta'(0)$ for different values of Pr in the presence of nanoparticles when $\gamma \to \infty$.

		Ref. [20]		Present results	
N_t	N_b	$-\theta'(0)$	$-\phi'(0)$	$-\theta'(0)$	$-\phi'(0)$
0.3	0.3	0.33984	1.83994	0.33984	1.83994
0.5	0.3	0.24088	1.95813	0.24088	1.95813
0.3	0.5	0.14814	1.87029	0.14814	1.87029
0.5	0.5	0.10478	1.94565	0.10478	1.94565

Table 5. Comparison of values of $-\theta'(0)$ for different values of Pr in the absence of nanoparticles when $\gamma \to \infty$.

Pr	Ref. [20]	Ref. [41]	Present results
0.07	0.066	0.0663	0.0663
0.20	0.169	0.1691	0.1691
0.7	0.454	0.4539	0.4539
2.0	0.911	0.9113	0.9113

6. Conclusions

The present study addresses the boundary layer flow of Carreau nanofluid over a stretching surface with convective boundary condition. The main points of this study are listed below.

(1) Influences of material parameter and power law index on the velocity are similar.
(2) An increase in the value of Prandtl number Pr reduces the temperature and concentration.
(3) Both temperature and thermal boundary layer thickness increase for larger γ. The heat transfer effects are not present when $\gamma = 0$.
(4) An increase in thermophoresis and Brownian motion parameter gives rise to the temperature and thermal boundary layer thickness.
(5) Brownian motion parameter has reverse effects on the temperature and concentration.
(6) Skin friction coefficient enhances through the increase in material parameter.
(7) Magnitude of local Sherwood number $-\phi'(0)$ is enhanced when Brownian motion parameter increases.
(8) Influence of the Brownian motion parameter and Lewis number on local Nusselt and Sherwood numbers are similar in a qualitative sense.

References

[1] S Kakac and A Pramuanjaroenkij, *Int. J. Heat Mass Transfer* **52**, 3187 (2009)
[2] S U S Choi, *ASME Int. Mech. Eng.* **66**, 99 (1995)
[3] S U S Choi, Z G Zhang, W Yu, F E Lockwood and E A Grulke, *Appl. Phys. Lett.* **79**, 2252 (2001)
[4] K Khanafer, K Vafai and M Lightstone, *Int. J. Heat Mass Transfer* **46**, 3639 (2003)
[5] H U Kang, S H Kim and J M Oh, *Exp. Heat Transfer* **19**, 181 (2006)
[6] M Turkyilmazoglu, *Chem. Eng. Sci.* **84**, 182 (2012)
[7] L Zheng, C Zhang, X Zhang and J Zhang, *J. Franklin Institute* **350**, 990 (2013)
[8] C Zhang, L Zheng, X Zhang and G Chen, *Appl. Math. Comput.* **39**, 165 (2015)
[9] M M Rashidi, S Abelman and N F Mehr, *Int. J. Heat Mass Transfer* **62**, 515 (2013)
[10] M Mustafa, J A Khan, T Hayat and A Alsaedi, *IEEE Trans.* **14**, 159 (2015)
[11] S A Shehzad, F M Abbasi, T Hayat and F Alsaadi, *PLoS One* **9(11)**, e111417 (2014)
[12] M Sheikholeslami, M G Bandpy and K Vajravelu, *Int. J. Heat Mass Transfer* **80**, 16 (2015)
[13] M Sheikholeslami, M Hatami and G Domairry, *J. Taiwan Inst. Chem. Eng.* **46**, 43 (2015)

[14] M Turkyilmazoglu, *ASME J. Heat Transfer*, DOI:10.1115/1.4025730
[15] M M Rashidi, N V Ganesh, A K A Hakeem and B Ganga, *J. Mol. Liquids* **198**, 234 (2014)
[16] L J Crane, *Z. Angew Math. Mech.* **21**, 645 (1970)
[17] T Hayat, M Waqas, S A Shehzad and A Alsaedi, *Scientia Iranica B* **21**, 682 (2014)
[18] S Mukhopadhyay, G C Layek and S A Samad, *Int. J. Heat Mass Transfer* **48**, 4460 (2005)
[19] K Bhattacharyya and G C Layek, *Chem. Eng. Commun.* **197**, 1527 (2010)
[20] W A Khan, M Khan and R Malik, *PLoS One* **9**, e105107 (2010)
[21] A Aziz, *Commun. Nonlin. Sci. Numer. Simulat.* **14**, 1064 (2009)
[22] R C Bataller, *Appl. Math. Comput.* **206**, 832 (2008)
[23] A Ishak, *Appl. Math. Comput.* **217**, 837 (2010)
[24] O D Makinde and A Aziz, *Int. J. Thermal. Sci.* **50**, 1326 (2011)
[25] T Hayat, M Waqas, S A Shehzad and A Alsaedi, *J. Mech.* **29**, 403 (2013)
[26] T Hayat, S Asad, M Mustafa and A Alsaedi, *Appl. Math. Comput.* **246**, 12 (2014)
[27] N Ali and T Hayat, *Appl. Math. Comput.* **193**, 535 (2007)
[28] B I Olajuwon, *Thermal. Sci.* **15**, 241 (2011)
[29] M S Tshehla, *Int. J. Phys. Sci.* **6**, 3896 (2011)
[30] S J Liao, *Beyond perturbation: Introduction to homotopy analysis method* (Chapman and Hall, CRC Press, Boca Raton, 2003)
[31] S J Liao, *Commun. Nonlin. Sci. Numer. Simulat.* **14**, 983 (2009)
[32] M M Rashidi, S A Mohimanian Pour, T Hayat and S Obaidat, *Comput. Fluids* **54**, 1 (2012)
[33] M Ghanbari, S Abbasbandy and T Allahviranloo, *Appl. Comput. Mech.* **12**, 355 (2013)
[34] M Turkyilmazoglu, *Commun. Nonlin. Sci. Numer. Simulat.* **17**, 4097 (2012)
[35] S Abbasbandy, E Shivanian and K Vajravelu, *Commun. Nonlin. Sci. Numer. Simulat.* **16**, 4268 (2011)
[36] O A Bég, M M Rashidi, N Kavyani and M N Islam, *Int. J. Appl. Math. Mech* **9**, 37 (2013)
[37] M Turkyilmazoglu, *Phys. Scr.* **86**, 015301 (2012)
[38] S Abbasbandy and T Hayat, *Commun. Nonlin. Sci. Numer. Simulat.* **14**, 3591 (2009)
[39] S A Shehzad, A Alsaedi, T Hayat and M S Alhuthali, *J. Taiwan Inst. Chem. Eng.* **45**, 787 (2014)
[40] S A Shehzad, A Alsaedi and T Hayat, *Int. J. Heat Mass Transfer* **55**, 3971 (2012)
[41] A Alsaedi, M Awais and T Hayat, *Commun. Nonlin. Sci. Numer. Simulat.* **17**, 4210 (2012)